J. Astrophys. Astr. (2018) 39:32
https://doi.org/10.1007/s12036-018-9526-5
© Indian Academy of Sciences

Higher-speed coronal mass ejections and their geoeffectiveness

A. K. SINGH*, ASHEESH BHARGAWA & APEKSHA TONK

Department of Physics, University of Lucknow, Lucknow 226 007, India.
*Corresponding author. E-mail: aksphys@gmail.com

MS received 25 October 2017; accepted 26 April 2018; published online 7 May 2018

Abstract. We have attempted to examine the ability of coronal mass ejections to cause geoeffectiveness. To that end, we have investigated total 571 cases of higher-speed (> 1000 km/s) coronal mass ejection events observed during the years 1996–2012. On the basis of angular width (W) of observance, events of coronal mass ejection were further classified as front-side or halo coronal mass ejections (W = 360°); back-side halo coronal mass ejections (W = 360°); partial halo (120° < W < 360°) and non-halo (W < 120°). From further analysis, we found that front halo coronal mass ejections were much faster and more geoeffective in comparison of partial halo and non-halo coronal mass ejections. We also inferred that the front-sided halo coronal mass ejections were 67.1% geoeffective while geoeffectiveness of partial halo coronal mass ejections and non-halo coronal mass ejections were found to be 44.2% and 56.6% respectively. During the same period of observation, 43% of back-sided CMEs showed geoeffectiveness. We have also investigated some events of coronal mass ejections having speed > 2500 km/s as a case study. We have concluded that mere speed of coronal mass ejection and their association with solar flares or solar activity were not mere criterion for producing geoeffectiveness but angular width of coronal mass ejections and their originating position also played a key role.

Keyword. Coronal mass ejections—geomagnetic storms—solar flares—geoeffectiveness—solar activity.

1. Introduction

Large structures containing plasma and magnetic fields are expelled from the Sun into the heliosphere and have the ability to cause geomagnetic storms (Gosling *et al.* 1990, Singh *et al.* 2014) are known as Coronal mass ejections (CMEs) and are one of the key parameter responsible for space weather problems (Singh and Singh 2003, Singh *et al.* 2010). After their first detection in the year 1971 (Tousey 1973), CMEs have posed the severe threat for dynamic and variable conditions in upper atmosphere. The enormous explosions of materials from the corona of the Sun are responsible for significant inputs of energy into our magnetosphere. Because the Sun can eject matter in any direction, only some of the CMEs are actually directed towards the Earth. CMEs responsible for the generation of geomagnetic storms have ability to produce geoeffectiveness and can be measured in terms of disturbed storm time index (Dst index). The main criteria for CMEs to cause geoeffectiveness are the condition that CMEs must arrive at Earth and also have a southward component of their magnetic field. Various studies have been carried out to deal with the properties of geoeffective CMEs and several attempts have been made to construct geomagnetic storm prediction-models based on the remotely-measured properties of CMEs (Srivastava 2005, Valach *et al.* 2009, Kim *et al.* 2010).

The occurrence of CMEs depends on the phase of the solar cycle. During solar maximum, CMEs originate from active regions and their occurrence rate may be 2/3 a day. While during solar minimum, CMEs form primarily in the coronal streamer belt near the solar magnetic equator and the occurrence rate may be one CME per week (Gopalswamy *et al.* 2003, 2007). CMEs occurring close to the disk center often to surround the occulting disk of the coronagraph with width 360° are known as halo CMEs (Howard *et al.* 1982). Halo CMEs can be front-sided and back-sided. Halo CMEs are fast and wide on the average and are associated with flares of greater X-ray importance because only energetic CMEs expand rapidly to appear above the occulting disk (Gopalswamy *et al*. 2007). CMEs with apparent widths between 120° and 360° are knows as partial halo CMEs

and those having angular width $< 120°$ are known as non-halo CMEs. Kim *et al.* (2005) investigated 305 CMEs (during the period 1997 to 2003) that included full ($W = 360°$) and partial halos ($120° < W < 360°$) and found that 121 of them were geoeffective. On the other hand, Gopalswamy *et al*. (2007) studied 378 full halos for the period 1996 to 2005 but they did not include partial halos and non-halo in their study. In our study, we have included full ($W = 360°$), partial halo ($120° < W < 360°$) and non-halo CMEs ($W < 120°$).

In the present study, we have considered CMEs having speed above 1000 km/s only and have examined the association of CMEs with various classes of solar flares and geomagnetic storms measured in terms of Dst index. As a case study, we have also considered CMEs having speed more than 2500 km/s. On the basis of these observational results, we have tried to establish correlation of geoeffectiveness with various categories of CMEs, solar flares and geomagnetic storms.

2. Data sources and selection criteria

CMEs data are extracted from the website of Solar and Heliospheric Observatory mission's Large Angle and Spectrometric Coronagraph (http://cdaw.gsfc.nasa.gov/CME_list) as compiled in the CME catalog (Yashiro *et al.* 2004, Gopalswamy *et al.* 2009). We have adopted the CMEs speed, class of solar flares and the CMEs locations from the same catalog for the period 1996–2012 (solar cycle 23 and half period of solar cycle 24). The CME catalog also defines halo and partial CMEs (Yashiro *et al.* 2004). Halo CMEs originating on the visible hemisphere represent ejection directed towards the Earth, and thus may cause the severest terrestrial consequences (Howard *et al.* 1982). In our observations, we have considered CMEs events having speed more than 1000 km/s (this speed is chosen randomly). We have examined total 571 cases of CMEs out of which 216 cases belong to the category of full halo CMEs (137 cases of front-side halo and 79 cases of back-side halo), 138 cases of partial halo CMEs and 217 cases of non-halo CMEs.

Coronal mass ejections (CMEs) which are usually triggered by solar flares produce radiation across the electromagnetic spectrum as well as a proton storm. Many CMEs are associated with solar flares but many are not, just as most flares are not associated with mass ejection. When CMEs and flares occur together, the CME onsets seem to precede the flares in many cases. The data for solar flares are taken from the website (http://www.ngdc.noaa.gov/stp/space-weather/solar-data/solar-features/solar-flares/X-ray/goes/). For present study we have classified geomagnetic storms with respect to their Dst magnitude in two categories: (i) moderate ($-50 > \text{Dst} \geq -100$ nT) and (ii) intense ($\text{Dst} < -100$ nT). Dst index data are extracted from the website of world data centre, i.e., http://wdc.kugi.kyoto-u.ac.jp/dstdir/index.html.

2.1 *Sources identifications for halo, partial halo and non-halo CMEs*

We have examined the characteristics of the front-side/back-side activity associated with the halo CMEs. We have found 137 cases of front-sided halo CMEs in which 51 CMEs were associated with X class flares, 66 with M class flares, 18 with C class flares, 1 with B class flare and 1 CME was not associated with any flare. Back-sided halo CMEs of 79 events were not associated with flares. It revealed that front-sided halo CMEs are mostly associated with big flares.

We have investigated 138 observed cases of partial halo CMEs, in which 12 cases were associated with X-class flares, 48 with M-class flares, 40 with C-class flares, 8 with B-class flares and 30 CMEs were not associated with any flare. For non-halo CMEs, 217 cases were investigated in this category out of which only 5 CMEs were associated with X class flares. The rest 33 cases of CMEs were associated with M class flares, 80 with C class flares, 18 with B class flares and 81 CMEs were not associated with flare. This has indicated that most of the non-halo CMEs might be associated with small class of flares or even not associated with any flare.

3. Association with solar flares

Solar flares and coronal mass ejections are the main drivers of the space weather effects in geo-space (Singh *et al.* 2010). The relationship between solar flares and CMEs are found to be very complex in nature and extensive efforts have been made so far to understand the causal relationship between these two transients. Sometimes there can be a solar flare without a CME and sometimes there can be CME without solar flare. CMEs activities have been associated with active features like solar flares and prominences. As the association of CMEs with solar flares is concerned, about 40% of solar flares do not have CMEs associated with them (Andrews 2003). Harrison (1991) investigated the temporal relationship between CMEs and flares and concluded that the CME onset typically precedes the associated X-ray

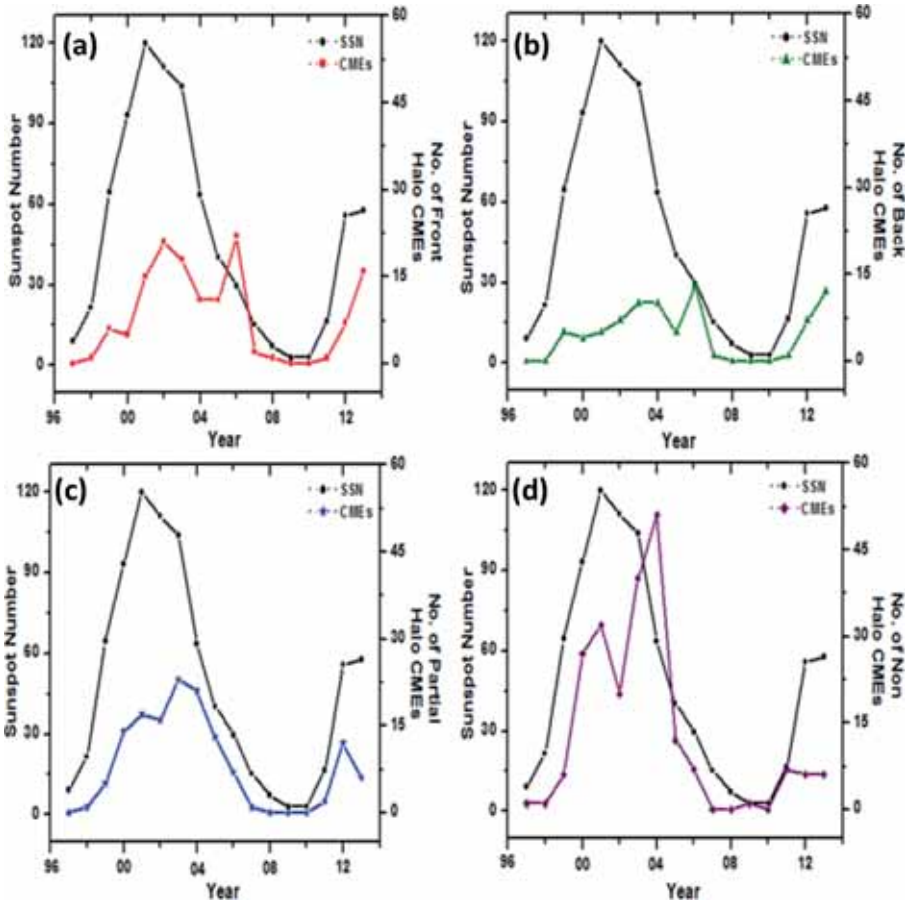

Figure 1. The occurrence number of halo CMEs (in various categories) and their variation with sunspot numbers.

flare onset by several minutes while Hundhausen (1999) claimed that this observational fact is not responsible for flares to produce CMEs. In this paper we have studied total 571 cases of observed CMEs in which 418 were accompanied by flares. For 153 (26.8%) cases of the CMEs flares were absent.

4. Geoeffectiveness of higher-speed CMEs

Solar activity plays a key role in production of various solar transients (Singh *et al.* 2010, Singh and Tonk 2014). In Fig. 1 we have plotted the variation of occurrence number of faster front-sided, back-sided, partial halo and non-halo CMEs with sunspot numbers for their comparison. The figure itself revealed that activity of halo CMEs were substantially dependent on solar activity, but there were other parameters which were responsible for the occurrence of faster halo CMEs and their tendency to show geoeffectiveness. As CMEs erupt from the Sun, particles with high speed and strong magnetic fields can hurl earthward causing a significant impact on the near-Earth space environment and produce geomagnetic storms (Singh *et al.* 2010, 2014). In fact, only CMEs having a significant earthward velocity component and directed towards the Earth can produce geomagnetic storms. Numerous severe storms occur during the maximum phase of the solar cycle and are mostly associated with CMEs with higher speed (Gopalswamy *et al.* 2007, Zhang *et al.* 2007, Singh *et al.* 2010, 2014). Some CMEs directed towards the Earth and observed as halos by spacecraft on the Sun-Earth line like SOHO, provide the key link between solar eruptions and major space weather phenomena such as geomagnetic storms and solar energetic particle events (Singh *et al.* 2010). So geoeffectiveness of halo CMEs depends on the source location on the disk. CMEs that are aligned near the relative disk center tend to be more geoeffective while those nearer the relative solar limb are less geoeffective. Halo CMEs appear to be faster and more energetic than non-halo CMEs (Gopalswamy *et al.* 2010a). The source regions of front-side halo CMEs are likely to be located within a few tens of degrees of Sun center from

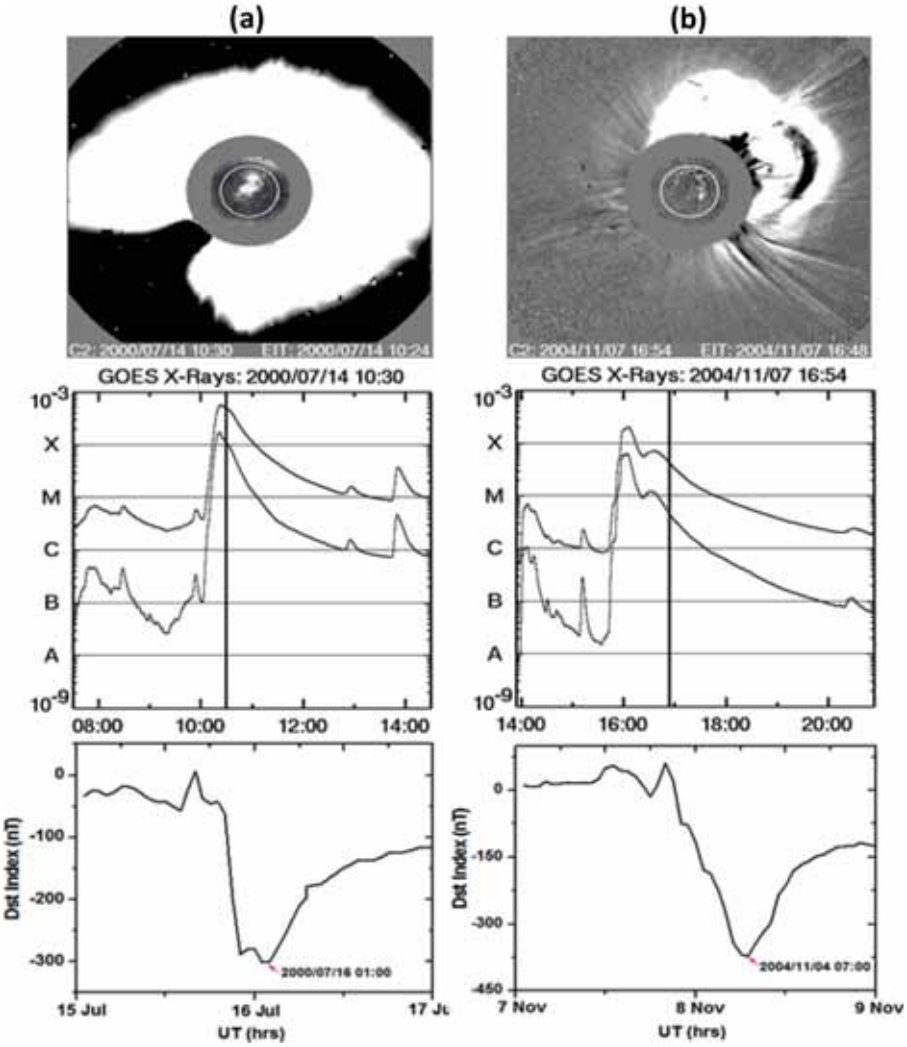

Figure 2. Typical examples of front-sided halo CMEs (**a**) observed on July 14, 2000 and (**b**) observed on November 7, 2004 with their respective occurrence time of CMEs, flares and geomagnetic storms.

the perspective of the observer (Cane *et al.* 2000, Webb 2002, Gopalswamy *et al.* 2010b).

4.1 *Geoeffectiveness of halo, partial-halo and non-halo CMEs*

We investigated 216 cases of halo CMEs (including back-sided) having speed more than 1000 km/s. 137 cases were observed as front-sided halo CMEs and 79 cases belonged to back-sided halo CMEs. Total 2604 cases of geomagnetic storms were observed due to halo CMEs, out of which 1971 cases were of moderate storm ($-50\,\text{nT} > \text{Dst} \geq -100\,\text{nT}$) category and 633 cases were intense storm ($\text{Dst} < -100\,\text{nT}$) category.

Due to front-sided halo CMEs, 2244 cases of geomagnetic storms were examined in which 1638 cases belonged to moderate category and 606 cases of intense storm. Two typical examples related to geoeffectiveness of front halo CMEs are depicted in Fig. 2a and b. Figure 2a revealed that front halo CME occurred on July 14, 2000 at 10:54 UT as a result of X1.0 class flare at 10:03 UT. This CME caused the geomagnetic storm of July 16, 2000 at 01:00 UT having Dst index − 301 nT. Further, the speed of this CME was observed as 1674 km/s. Similarly, Fig. 2b revealed that the front halo CME occurred on November 7, 2004 at 16:54 UT as a result of X5.7 class flare and this was responsible for the geomagnetic storm of November 8, 2004 at 07:00 UT having Dst index − 374 nT. The CME speed in this case was recorded as 1759 km/s.

For back-sided halo CMEs, we have investigated 360 cases of geomagnetic storms, out of which 333 cases belonging to moderate storm category and only 27 cases of intense storm category. Figure 3a and b depict two

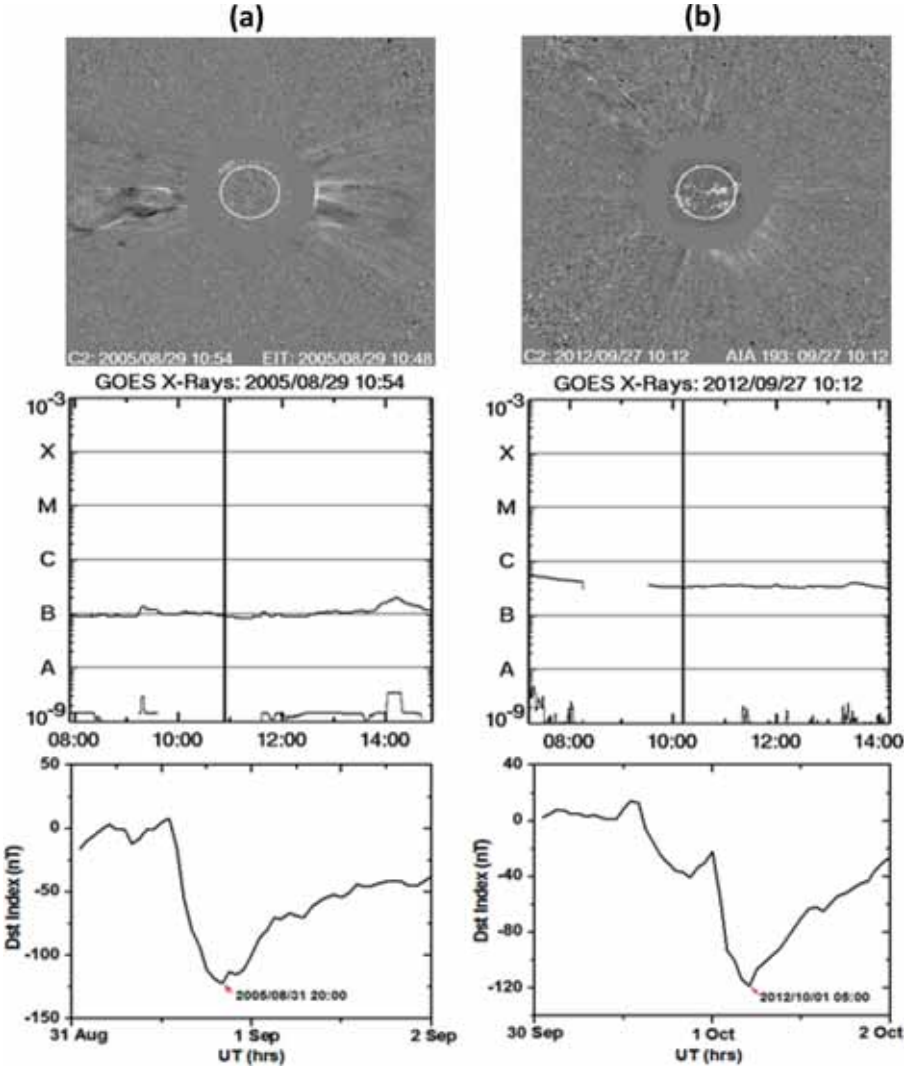

Figure 3. Depiction of Back-sided halo CMEs (**a**) observed on August 29, 2005 and (**b**) observed on September 27, 2012 with their respective occurrence time of CMEs, flares and geomagnetic storms.

typical examples of back-sided halo CMEs. Figure 3a revealed that on August 29, 2005 back-sided halo CME occurred at 10:54 UT with speed 1600 km/s and it caused geomagnetic storm on August 31, 2005 at 22:00 UT having Dst index − 122 nT. No flare was observed during this event. Similarly, Fig. 3b revealed that back-sided halo CME was observed on September 27, 2012 at 10:23 UT with speed 1319 km/s and caused geomagnetic storm of October 1, 2012 at 24:00 UT with Dst index − 119 nT.

During our investigation, total 138 cases of partial halo CMEs were observed. Total 1139 cases of geomagnetic storms were observed in which 872 cases were of moderate storm category, while 267 cases were of intense storm category. Figure 4 depicts two typical examples of partial halo CMEs. Figure 4a revealed that on April 20, 2001, partial halo CME was occurred at 10:06 UT with speed 1160 km/s and caused a geomagnetic storm on April 22, 2001 at 16:00 UT. A flare of class C1.5, preceding the CME onset, was observed on the same day. The reason for this is that on the same day another strong flare was occurred and that had no connection with above CME. Figure 4b shows that another case of partial halo CME was occurred on May 27, 2003 at 22:06 UT with speed 1122 km/s caused the geomagnetic storm of May 29, 2003 at 24:00 UT with Dst index − 144 nT.

For non-halo CMEs, 217 cases were examined for present study. We have found total 1819 cases of geomagnetic storms were recorded due to non-halo CMEs in which 1430 cases were of moderate storm category and 389 cases were of intense storm. Figure 5 depicts

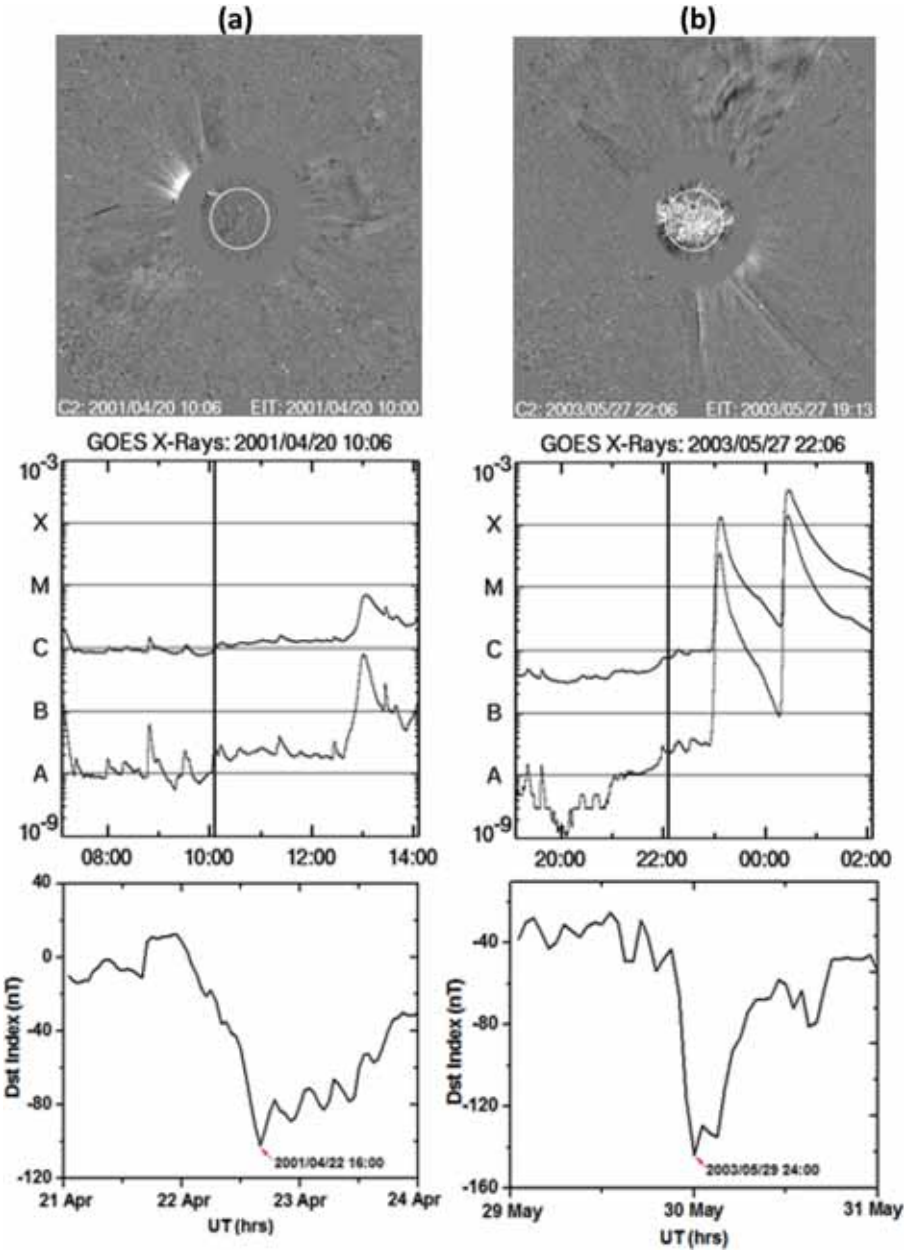

Figure 4. Depiction of CMEs occurrence with, flares and geomagnetic storms as an example of partial halo CMEs.

two typical examples of non-halo CMEs observed during the investigating period of 1996–2012. Figure 5a revealed that on October 18, 1999 a non-halo CME occurred at 02:06 UT having speed 1081 km/s and caused geomagnetic storm on October 22, 1999 at 07:00 UT of Dst index − 237 nT. Flare of class C2.8 was also recorded on October 18. Similarly, Fig. 5b revealed that a non-halo CME occurred on March 30, 2001 at 03:36 UT having speed 1072 km/s that caused geomagnetic storm on March 31, 2001 at 09:00 UT. Flare of class C7.5 was recorded on March 30 at 02:20 UT.

5. Superfast (speed > 2500 km/s) CMEs events: a case study

During our analysis of fast CMEs (speed > 1000 km/s), we noticed 11 events of CMEs having speed more than 2500 km/s. Out of these 8 CMEs were of front halo, 2 back-side halo CMEs and 1 partial halo CMEs. Table 1 provides the detailed information of the same. The first event of a full front-side halo CME (360° angular widths) category having speed 2519 km/s was observed on November 25, 2000 at 01:32 UT. The CME was originated from the position N07E50 where an M8.2 class

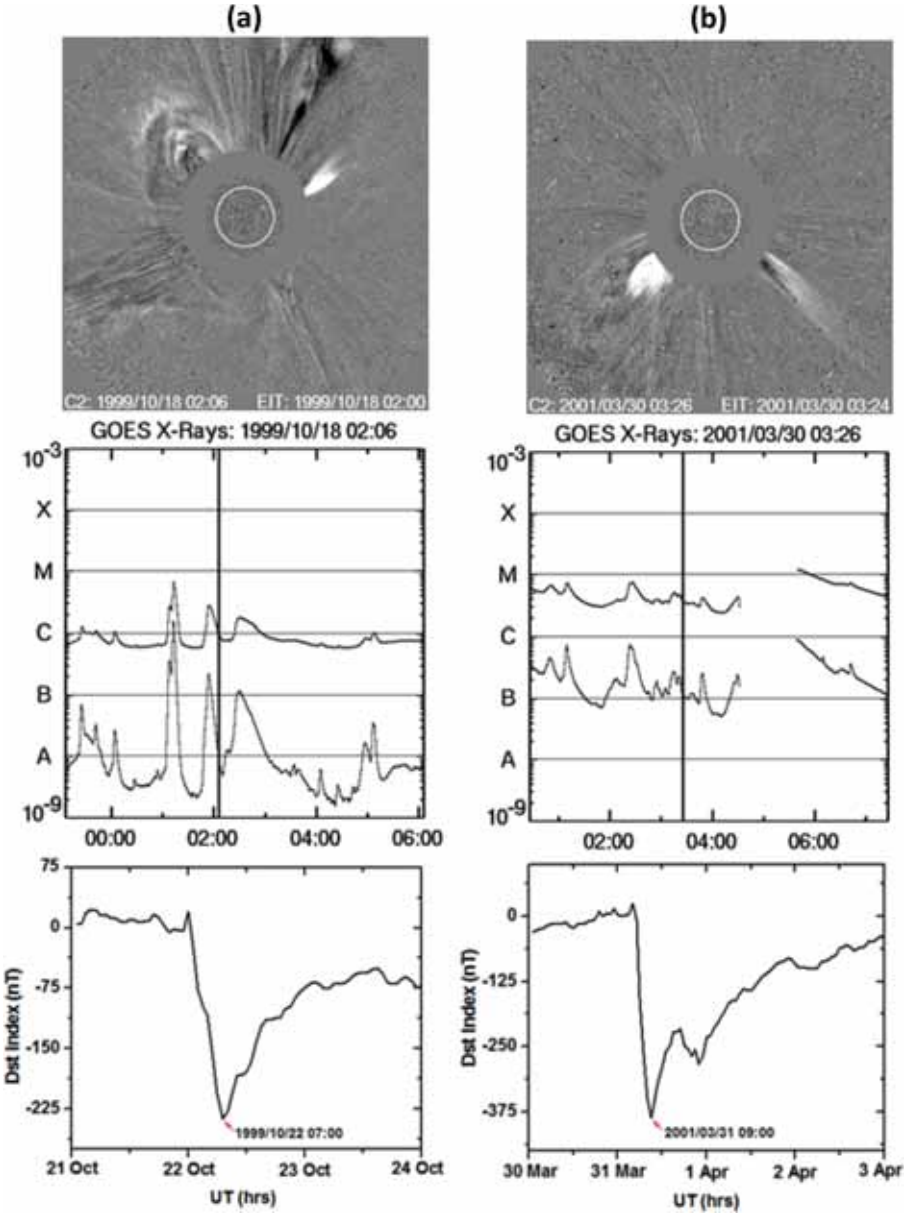

Figure 5. Depiction of CMEs occurrence, flares and geomagnetic storms as an example of nonhalo CMEs.

Table 1. Eleven cases of Superfast CMEs events, their occurrence time, and associated flares and geomagnetic storms.

CME types	Year	Date and month	Occurrence time (UT)	Speed (km/s)	Solar Flare class	Dst Index
Front halo	2000	25 Nov	01:31:58	2519	M8.2	− 127
	2003	2 Nov	17:30:05	2598	X8.3	− 69
		4 Nov	19:54:05	2657	X28	− 69
	2004	10 Nov	02:26:05	3387	X2.5	− 263
	2005	15Jan	23:06:05	2861	X2.6	− 103
		17 Jan	09:54:05	2547	X3.8	− 103
	2012	27 Jan	18:27:52	2508	X1.7	No storm
		7 Mar	00:24:06	2684	X5.4	− 131
Back-sided halo	2000	12 May	23:26:05	2604	C6.6	− 92
	2005	24 Jul	13:54:05	2528	No flare	No storm
Partial halo	2001	02 Apr	22:06:07	2505	X20.0	No storm

flare occurred and produced an intense storm (Dst = −127 nT) on November 29, 2000. This CME was observed in LASCO C2 and C3 as a halo CME (most prominent in the northeast quadrant). Another event of a full front-side halo CME having speed 2598 km/s was observed on November 2, 2003. The originating position was S14W56 while it was followed by X8.3 class of flare and produced a moderate storm (Dst = −69 nT) on November 4, 2003. This CME was most prominent in the southwest quadrant. The third event of superfast CME was observed on November 4, 2003 having speed 2657 km/s. This originated from the position S19W83 where an X28 flare occurred and produced a moderate storm (Dst = −69 nT) on November 4, 2003. The CME was also most prominent in the southwest quadrant. The next event of this category appeared on November 10, 2004 having speed of 3387 km/s and originated from the position N09W49 where an X2.5 class flare occurred. This event was observed in LASCO C2 and C3 as a halo CME (most prominent in the northwest quadrant). Since a severe storm (Dst = −263 nT) was recorded on the same day; this may be because of some other CMEs.

The fifth event of this category was observed on January 15, 2005 with speed of 2861 km/s. This originated from the position N15W05 where an X2.6 class flare was observed and it produced an intense storm on January 18, 2005 with Dst (− 103 nT). This CME was prominent in the northwest quadrant. The next event of the CME in this category was observed on January 17, 2005 having speed 2547 km/s and originated from the position N15W25 where an X3.8 class flare occurred and was responsible to produce an intense storm (Dst = −103 nT) and the CME was also most prominent in the northwest quadrant. The seventh event of this category appeared as a full front-side halo CME on January 27, 2012 having speed 2508 km/s and originated from the position N27W71 where an X1.7 class flare occurred, but surprisingly there was no storm. This CME was also most prominent in the northwest quadrant. The last (eighth) event of this category was observed on March 7, 2012 having speed 2684 km/s. It originated from the position N17E27 where an X5.4 class flare occurred and produced an intense storm (Dst = −131 nT) on March 9, 2012. This halo CME was also most prominent in the northeast quadrant.

Two events of full back-sided superfast halo CMEs (360° angular widths) were observed during the analysis period 1996–2012. The first event was recorded on May 12, 2000 having speed 2604 km/s and this was responsible to produce moderate storm (Dst index = −92 nT) on May 17, 2000. The second event of a full back-sided superfast halo CME was recorded on July 24, 2005 with speed of 2528 km/s. The only event of superfast partial halo CME (261° angular widths) with speed 2505 km/s was observed on April 2, 2001 and was associated with an X20 class flare but there was no storm observed.

A typical comparison of each of the superfast front-sided halo, superfast back-sided halo and a superfast partial halo CMEs are shown in Fig. 6. Figure 6a reveals the event that includes halo CME flare and geomagnetic storm, Fig. 6b shows that there were CME but no flare or storm while Fig. 6c shows the event of CME and flare but no storm. Form this we have inferred that geo-effectiveness is not dependent of CME speed and their association with flares only but it might depend on the angular width and originating position of CMEs also.

6. Results and discussion

Halo CMEs had been reported infrequently during coronagraph observations of the Sun before SOHO mission (Howard *et al.* 1982). In coronagraphic observation, halo CMEs appear as enhancement surrounding the entire occulting disk looks like a roughly circular 'halo' surrounding the Sun. Halo only means that the CME source region is located centrally on the solar disk. This implies that a considerable part of the early CME evolution appears against the solar disk. The study of halo coronal mass ejections (CMEs) has become one of the principal areas of solar research (Hudson *et al.* 1998, Webb *et al*. 2000, Song *et al.* 2006, Temmer *et al.* 2008). Since halos became common place in the SOHO era, there have been several attempts to characterize their geoeffectiveness (Yermolaev and Yermolaev 2003, Zhao and Webb 2003, Kim *et al.* 2005, Yermolaev *et al*. 2005, Gopalswamy *et al*. 2007, Gopalswamy 2009). Using CMEs from the rise phase of solar cycle 23, St Cyr (2000) concluded that ∼ 75% of the front-sided CMEs are geoeffective. Now it is well accepted that the front-side halo CMEs are the major causes for geomagnetic storms (Cane *et al.* 2000, Wang *et al*. 2002, Zhang *et al.* 2003, Gopalswamy *et al*. 2007). Recently, Gopalswamy *et al.* (2014) and Selvakumaran *et al.* (2016) have compared the occurrence and speed of CMEs and geoeffectveness for solar cycles 23 and 24.

In the present paper we have examined the various characteristics of faster CMEs having speed above 1000 km/s and that were observed during last one and a half solar cycles (1996–2012). We have investigated front-sided halo CMEs, back-sided halo CMEs, partial halo CMEs and non-halo CMEs and the association of various categories of CMEs with flares and their geoeffectiveness. CMEs could be characterized

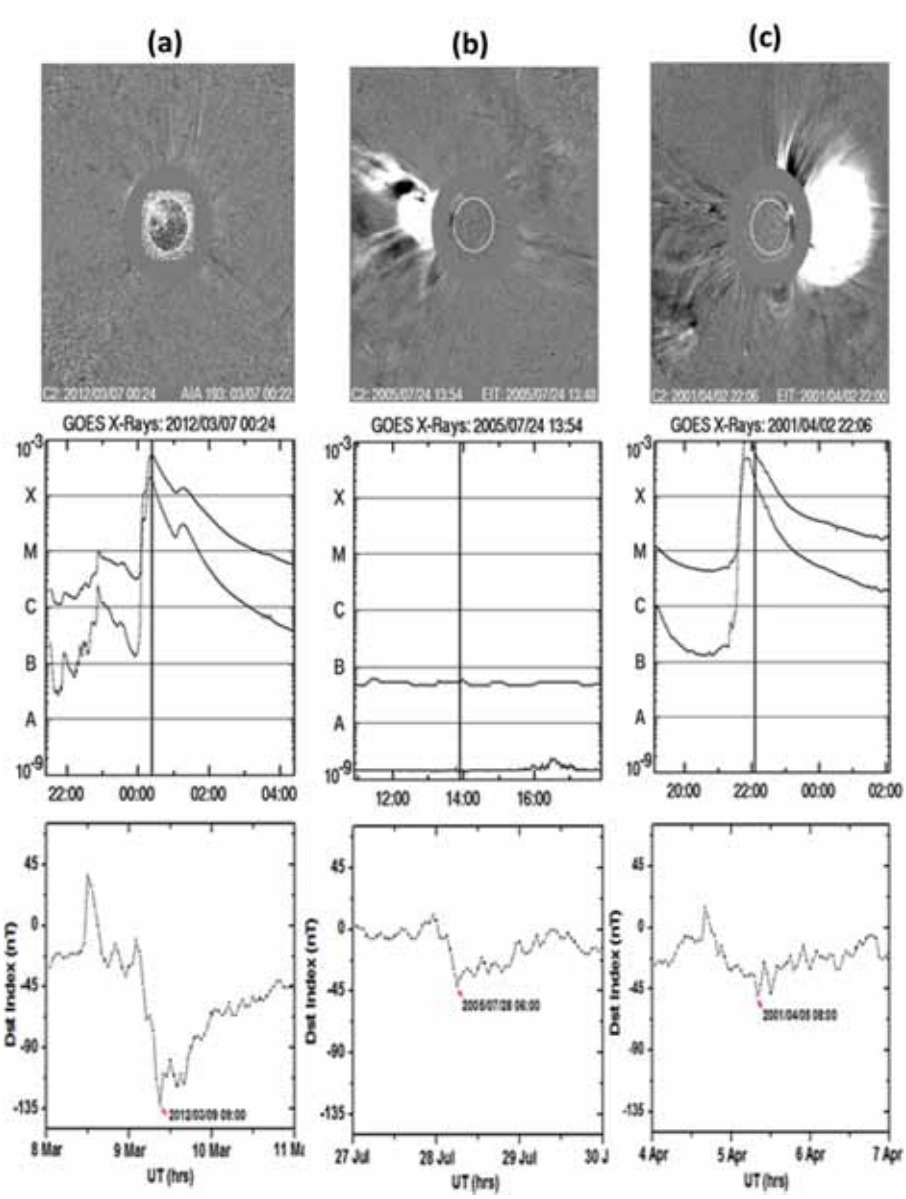

Figure 6. (**a**) Shows the event of halo CME with flare and geomagnetic storm, (**b**) shows the event of CME but no flare or storm, (**c**) shows the event of CME and flare but no storm.

by speed, angular width and central position angle in the sky plane. Out of 571 total cases analyzed, front-sided halo CMEs showed 67% geoeffectiveness, while back-sided halo CMEs showed 43% geoeffectiveness. Partial halo CMEs showed 44% geoeffectiveness and no halo CMEs showed 56% geoeffectiveness. Further, number of front-sided halo CMEs were mostly associated with X-class flares in comparison of back-sided halo and partial halo or non-halo CMEs respectively. As the association of CMEs with solar flares was concerned, about 40% of solar flares did not have CMEs associated with them (Andrews 2003). We have also noticed that 418 cases of CMEs were accompanied by flares while in 153 (26.8%) cases of CMEs flares were absent.

As a case study we have examined 11 (8 front-sided, 2 back-sided and 1 partial) events of superfast halo CMEs where their speed varied from 2505 km/s to 3387 km/s. One thing was common that all these events had occurred during higher solar activity periods. Nine events were associated with flares, while one event recorded on January 27, 2012 and having speed 2508 km/s did not show any association with flare. In case of one event observed on July 24, 2005 having speed 2528 km/s and originated from the east quadrant of B-limb, there was no flare and no storm recorded.

In the above observations it could be noticed that in three events no storm observed while in rest of the eight events they had shown only moderate and intense storm while not a single case was observed as great or super storm. This inferred that even CMEs having fastest of the speed they may not produce geomagnetic storms or in other words they did not show geoeffectiveness. On the basis of the above facts, we have inferred that CMEs association with flares and their higher speed were not the only criterion to produce geoeffectiveness. Even the high solar activity conditions were not sufficient to produce geoeffectiveness. Geoeffectiveness of faster CMEs were associated with angular width, originating position, flares, speed and solar activity as a whole.

7. Conclusions

Total 571 events of higher-speed (> 1000 km/s) CMEs belonging to front-sided halo, back-sided halo, partial halo and non-halo categories were examined and their association with flares and geoeffectiveness were tested. Front-sided halo CMEs showed 67% geoeffectiveness, while back-sided halo CMEs showed 43% geoeffectiveness. Partial halo and non-halo CMEs showed their effectiveness at 44% and 56% respectively. Here geoeffectiveness of non-halo CMEs were substantial, possibly due to our consideration of faster speed. We have concluded that the variation in the number of fast CMEs was well correlated with the solar cycle where front-sided halo CMEs show more geoeffectiveness than partial halo and non-halo CMEs. Back-sided halo CMEs were much less geoeffective in comparison of above categories of CMEs. There was a significant difference between the flare association of front-sided halo CMEs and back-sided halo CMEs. Front-sided halo CMEs were mostly associated with big flares and back-sided halo CMEs were associated with small flares or not associated with any flare. Also the speed of non-halo CMEs were less than partial halo and full halo CMEs because we have not observed any non-halo CMEs speed more than 2300 km/s. We have concluded that the geoeffectiveness did not depend upon the speed and angular width of CMEs only but on the position of CMEs, i.e. whether the positions of CMEs were front-sided or back-sided. In our study, there were many CMEs which were not associated with any flare. There were differences between the flare association of partial halo and full halo CMEs because it (flare association) was dependent on the angular width and position of CMEs while CMEs speed did not depend upon the size of flares.

Acknowledgements

AKS is thankful to Indian Space Research Organization (ISRO) for providing financial support for the present work under CAWSES India phase II program.

References

Andrews M. D. 2003, Sol. Phys., 218, 261
Cane H. V., Richardson I. G., St Cyr O. C. 2000, Geophys. Res. Lett., 27, 3591
Gopalswamy N., Lara A., Yashiro S., Nunes S., Howard R.A. 2003, in Proceedings of ISCS 2003 Symposium on Solar Variability as an Input to Earth's Environment. Eur. Space Agency Spec. Publ. ESA-SP, 535, 403
Gopalswamy N., Yashiro S., Akiyama S. 2007, J. Geophys. Res., 112, A06112
Gopalswamy N. 2009, Earth Moon Planets 61, 1
Gopalswamy N., Yashiro S., Michalek G., Stenborg G., Vourlidas A., Freeland S., Howard R. 2009, Earth Moon Planets 104, 295
Gopalswamy N., Yashiro S., Michalek G., Xie H., Makela P., Vourlidas A., Howard R. A. 2010a, Sun and Geosphere, 5, 7
Gopalswamy N., Xie H., Makela P., Akiyama S., Yashiro S., Kaiser M. L., Howard R. A., Bougeret J. L. 2010b, Appl. Phys. J., 710, 1111
Gopalswamy N., Akiyama S., Yashiro S., Xie H., Mäkelä P., Michalek G. 2014,Geophys.Res. Lett., 41, 2673
Gosling J. T., Bame S. J., McComas D. J., Phillips J.L. 1990, Geophy. Res. Lett., 17, 901
Harrison R. A. 1991, Adv. Space Res., 11, 25
Howard R. A., Michels D. J., Sheeley Jr N. R., Koomen M. J. 1982, Astrophys J., 263, L101
Hudson H. S., Lemon J. R., St Cyr O. C., Sterling A. C., Webb D. F. 1998, Geophys. Res. Lett., 25, 2481
Hundhausen A. J. 1999, Many faces of the Sun, Springer, New York, p. 143
Kim R. S., Cho K. S., Moon Y. J., Kim Y. H., Yi Y., Dryer M., Bong S. C., Park Y. D. 2005, J. Geophys Res., 110, A11104
Kim R. S., Cho K. S., Moon Y. J., Dryer M., Lee J., Kim K. H., Wang H., Park Y. D., Kim Y. H. 2010, J. Geophys Res., 115, A12108
Selvakumaran R., Veenadhari B., Akiyama S., Pandya M., Gopalswamy N., Yashiro S., Kumar S., Mäkelä P., Xie H. 2016, J. Geophys. Res. Space Physics, 121, https://doi.org/10.1002/2016JA022885
Singh A. K., Singh R. P. 2003, Ind. J. Phys., 77, 611
Singh A. K., Tonk A. 2014, Astrophys Spac Sci., 352(2), 367

Singh A. K., Siingh D., Singh R. P. 2010, Surv. Geophys., 31, 581
Singh A. K., Tonk A., Singh R. 2014, Ind. J. Phys., 88(11), 1127
Song H., Yurchyshyn V., Yang G., Chen C. W., Wang H. 2006, Sol. Phys. 238, 141
Srivastava N. 2005, Ann. Geophys., 23, 2929
St Cyr O. C. 2000, J. Geophys Res., 105, 18169
Temmer M,. Vergoing A. M., Vrsnak B., Rybak J., Gomory P., Stoiser S., Marricic D. 2008, Astrophys. J., 673, 95
Tousey R. 1973, The solar corona (Berlin: Akademie–Verlag) (eds.) Rycroft MJ, Runcorn SK, pp. 713–730
Valach F., Revallo M., Bochnicek J., Hejda P. 2009, Space Weather, 7, S04004
Wang J. L., Gong J. C., Liu S. Q., Le G. M., Sun J. L. 2002, Chin J Astr. Astrophys 2, 557
Webb D. F., Cliver E. W., Crooker N. U., St Cyr O. C., Thompson B. J. 2000, J. Geophys Res., 105, 7491
Webb D. F. 2002, in From Solar Min to Max: Half a Solar Cycle with SOHO, Proceedings of the SOHO 11 Symposium, 1–15 March 2002, Davos, Switzerland. A symposium dedicated to Bonnet RG (Ed.) Wilson A, vol. SP-508 of ESA Special Publications, pp. 409–419, ESA Publications Division, Noordwijk
Yashiro S., Gopalswamy N., Michalek G., St Cyr O.C., Plunkett S.P., Rich N.B., Howard R.A. 2004, J. Geophys Res., 109, A07105
Yermolaev Yu. I., Yermolaev M. Yu., 2003, Cosmic Res., 41, 539
Yermolaev Yu. I., Yermolaev M. Yu., Zastenker G. N., Zelenyi L. M., Petrukovich A. A., Sauvaud J. A. 2005, Planet Space Sci., 53, 189
Zhang J., Dere K. P., Howard R. A., Bothmer V. 2003, Astrophys J., 582, 520
Zhang J., Richardson I. G., Webb D. F., Gopalswamy N., Huttunen E., Kasper J. C., Nitta N. V., Poomvises W., Thompson B. J., Wu C. C., Yashiro S., Zhukov A. N. 2007, J. Geophys Res., 112, A10102
Zhao X. P., Webb D. F. 2003, J. Geophy. Res., 108(A6), 1234. https://doi.org/10.1029/2002JA009606